JOURNAL OF GEOPHYSICAL RESEARCH, VOL. 89, NO. B9, PAGES 7836-7844, SEPTEMBER 10, 1984

SHOCK WAVE EQUATIONS OF STATE USING MIXED-PHASE REGIME DATA

J. Peter Watt[1] and Thomas J. Ahrens

Seismological Laboratory, California Institute of Technology, Pasadena

Abstract. A method is given that uses Hugoniot data in the mixed-phase regime to constrain further equation of state (EOS) parameters of low- and high-pressure phases of materials undergoing phase transformations on shock loading. We compute the relative proportion of low- and high-pressure phases present in the mixed-phase region and apply additional tests to the EOS parameters of the separate low- and high-pressure phases by invoking two simple requirements: the fraction of high-pressure phase (1) must increase with increasing shock pressure, and (2) must approach one at the high-pressure end of the mixed-phase regime. We apply our analysis to previously published data for potassium thioferrite, $KFeS_2$, and pyrrhotite, $Fe_{0.9}S$. We find that including the mixed-phase regime data in the $KFeS_2$ analysis requires no change in the published high-pressure EOS parameters. For $Fe_{0.9}S$ we must modify the high-pressure phase EOS parameters to account for both the mixed-phase and high-pressure phase Hugoniot data. Our values of zero-pressure density, bulk modulus and first pressure derivative of the bulk modulus of the high-pressure phase of $Fe_{0.9}S$ are 5.3 Mg/m^3, 106 GPa, and 4.9, respectively.

Introduction

In shock wave experiments on materials that undergo phase transformations upon shock loading, low- and high-pressure portions of the pressure-density curves are separated by a region termed the "mixed-phase" regime, a range of compressions in which both phases are thought to coexist. Most attention in shock wave work in the past has been focused on either the low- or the high-pressure regime. In the former region, results of static compression studies can be compared to the dynamic results, while geophysicists' interest in the high-pressure regime arises from the possibility of elucidating the high-pressure behavior of possible mantle or core minerals. Examples are shock studies on pyroxene and olivine [McQueen et al., 1967; Jeanloz and Ahrens, 1977; Jackson and Ahrens, 1979; Watt and Ahrens, 1983], iron [Jeanloz, 1979], iron sulfide [Ahrens, 1979], and anorthite [Jeanloz and Ahrens, 1980]. The mixed-phase region is usually regarded as something of a nuisance, a pressure interval to be traversed as quickly as possible in order to reach the more interesting high-pressure regime.

Mixed-phase regime states can be detected with the various observing techniques currently in use in shock wave experiments: flash gap blocks, pin detectors, and plane or inclined mirrors mounted on the sample. With inclined mirrors any elastic and one or more deformational waves can be seen and the appropriate elastic or Hugoniot state can be determined. With the other methods only the wave (elastic or deformational) travelling in the sample with the highest velocity can be detected, and the question arises whether this wave denotes an elastic, mixed-phase, or high-pressure state. By computing a theoretical Hugoniot for the low-pressure phase from static compression, ultrasonic, or Brillouin scattering data, one can see at what point the shock wave data deviate from the low-pressure phase Hugoniot toward higher densities and thus decide whether the data lie in the mixed-phase or the high-pressure phase regime rather than in the elastic region.

Development of in-material stress wave measuring systems has enabled yielding and phase transformation processes to be studied as a shock wave progresses through a sample. Grady [1977, 1980] reviews various experimental techniques and discusses general features of shock loading and unloading. Such work has led to increased interest in the mixed-phase (mp) regime and, in particular, in the question of how materials under shock unload once the shock wave has passed.

Grady et al. [1974] measured release paths in the alpha-quartz/stishovite mp region using in-material manganin gages. They concluded that at a given Hugoniot density in the mp field, the material unloaded following "frozen concentration" paths (constant mass fractions of stishovite and quartz) down to pressures of about 8 GPa with the release paths becoming shallower as the amount of stishovite in the mp region decreased.

In this paper, we show how Hugoniot data from the mp region can be used to constrain further equation of state (EOS) parameters for the low- and high-pressure phases. As illustrations, we use previously reported data from the mp regimes of potassium thioferrite, $KFeS_2$ [Somerville and Ahrens, 1980] and pyrrhotite, $Fe_{0.9}S$ [Ahrens, 1979]. We also set up the mp release path problem in general terms, calculate theoretical release paths for the two materials above, and compare calculated and measured release paths.

Theory

For a given mp Hugoniot state we first calculate the amounts of low- and high-pressure phases in a manner similar to Ahrens et al. [1976] for olivine. We assume that both low- (lpp) and high-pressure (hpp) phase components in the mp region are at the same temperature. Accordingly, we combine lpp and hpp isotherms to match the observed mp densities at the mp Hugoniot pressure. We thus assume pressure, temperature, and particle velocity equilibrium between the two phases and ignore surface energy effects. In their study of coexisting alpha-quartz and stishovite, Grady et al. [1974] combined adiabats, noting that the

[1]Now at Department of Geology, Rensselaer Polytechnic Institute, Troy, New York.

Copyright 1984 by the American Geophysical Union.

Paper number 4B0741.
0148-0227/84/004B-0741$05.00

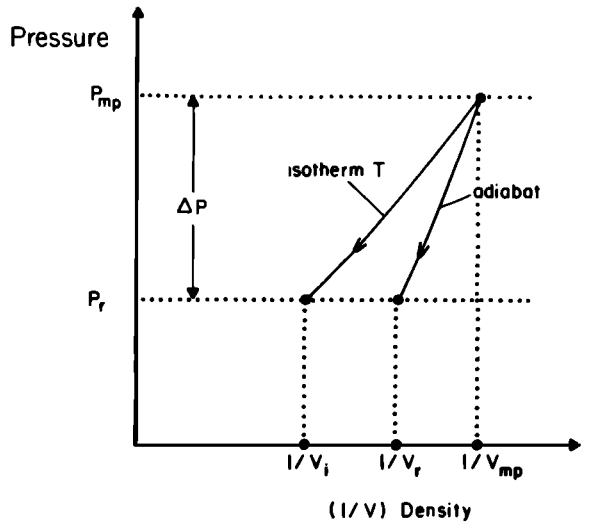

Fig. 1. Schematic adiabats and isotherms for low- (lpp) and high-pressure (hpp) phases used to calculate relative proportions of each component at a given Hugoniot pressure P in the mixed-phase (mp) regime from mass and energy balance conditions in equations (1) and (2).

difference between isotherms and adiabats is small; however, at a given pressure, temperatures on the lpp and hpp adiabats are generally different. We do the more rigorous analysis here. By assuming thermal equilibrium between the low- and high-pressure phases we also ignore thermal localization effects by which isolated high-temperature regions may serve as the nuclei for shock-induced phase transitions, as proposed by Grady [1980].

In a two-phase region, mass and energy balance considerations yield

$$V_{mp} = xV_h(P,T) + (1-x)V_\ell(P,T) \quad (1)$$

and

$$P(V_o-V_{mp})/2 = x[E_{tr} - \int_{V_{oh}}^{V_h} P_s dV + (P-P_{sh})V_{oh}(V_{oh}/V_h)^{n_h-1}/\gamma_{oh}] + (1-x)[-\int_{V_{o\ell}}^{V_\ell} P_s dV + (P-P_{s\ell})V_{o\ell}(V_{o\ell}/V_\ell)^{n_\ell-1}/\gamma_{o\ell}] \quad (2)$$

where x is the mass fraction of the high-pressure phase at mp pressure P and specific volume V_{mp}, V_o is zero-pressure specific volume, E_{tr} is the transition energy from the low- to high-pressure phase, γ_o is the zero-pressure Grüneisen parameter, n is the exponent relating Grüneisen parameter and specific volume assuming that $\gamma/\gamma_o = (V/V_o)^n$, P_s is the pressure on an adiabat at volume V, and the subscripts "ℓ" and "h" denote low- and high-pressure phase, respectively (Figure 1). Equation (2) corrects and generalizes to $n \neq 1$ equation (4) of Ahrens et al. [1976]. It equates the increase in energy at pressure P on the mp Hugoniot to the energy change along the adiabats of both phases plus the energy required to raise the pressure at constant volume from the adiabats to isotherms of temperature T and includes the transition energy E_{tr}.

We use third-order finite strain to calculate adiabats:

$$P_s = 1.5K_o y^{5/3}(y^{2/3}-1)[1 + B(y^{2/3}-1)] \quad (3)$$

where $y=V_o/V$, K_o is the zero-pressure bulk modulus, and $B=0.75(\partial K_o/\partial P-4)$. Pressures ($P_T$) on isotherms of temperature T are related to adiabat pressures by

$$P_T = P_s + \gamma_o C_v(T-T_s)v^{n-1}/V_o^n \quad (4)$$

where C_v is specific heat at constant volume (assumed constant). Temperature T_s on an adiabat is given by

$$T_s = T_o \exp\left(-\gamma_o[(V/V_o)^n-1]/n\right) \quad (5)$$

where T_o is the temperature of the unshocked material (300°K). In (4) and (5) we again assume that $\gamma/\gamma_o = (V/V_o)^n$.

The problem is then to find the lpp and hpp volumes V_ℓ and V_h so that the mass and energy balance equations (1) and (2) are satisfied at a set mp pressure P ($=P_T$). We substitute (3) and (5) into (4) to obtain an implicit equation for $P_T(y)$ for the individual low- and high-pressure phases on isotherm T, solve for y (i.e., for V_ℓ and V_h) using Newton's method, calculate x from (1), and check for energy balance using (2). We adjust the isotherm temperature T until (2) is satisfied to a specified tolerance. The parameters needed for each phase are $V_o(=1/\rho_o)$, K_o, $\partial K_o/\partial P$, γ_o, n, C_v, and E_{tr}.

For consistency among the lpp, hpp, and mixed-phase Hugoniot states the proportion of the hpp computed in the mp region must increase with increasing pressure and must approach unity at the high-pressure end of the mp regime. If these conditions are not met, then the EOS parameters must be adjusted until the conditions are satisfied. Thus mp region Hugoniot data can be included in the determination of EOS parameters for the lpp and hpp. This approach can also be used to refine initial estimates of the pressure limits of the mp regime, i.e., the pressures at which the values of x in (1) are 0 and 1. We illustrate this procedure below.

Once we have determined EOS parameters compatible with all the experimental Hugoniot states, including mp states, we calculate release adiabats. We assume that shocked materials unload isentropically. Kieffer and Delaney [1979] showed that if the work done against viscous forces in a material in a shock state is small compared with the gain in lattice strain energy upon adiabatic rarefaction, the effective viscosity of the material must be less than 10^3 kg/m s (10^4 poise). Jeanloz and Ahrens [1979] have argued that this condition is satisfied for many geological materials shocked to pressures below 150 GPa.

We assume that the amount of hpp remains constant while the sample unloads to zero pressure. This "frozen concentration" release adiabat is the steepest theoretical release path and yields the maximum theoretical postshock density. This can be compared with experimental release paths

determined using shock velocities in buffer mirrors mounted on shock-compressed samples [Ahrens et al., 1969], the impedance matching method, and an approximation to the Riemann integral for the release wave velocity [Rice et al., 1958; Lyzenga and Ahrens, 1978]. The pressure-particle velocity release path is assumed linear and is shown to be an extremum, which extremum is then inferred to yield a maximum value for postshock density.

We calculate the release adiabat iteratively, as follows. For both the lpp and hpp we consider the energy change produced by a small pressure decrement, treating both isothermal and adiabatic paths, starting from the mp Hugoniot pressure P_{mp}. Figure 2 illustrates the first iteration. The change in energy, ΔE_i, along isotherm T from P_{mp} to P_r is [Ahrens et al., 1969]

$$\Delta E_i = \Delta P(V_i - V_{mp})/2 + C_v T \gamma_o (V_i^n - V_{mp}^n)/n/V_o^n \quad (6)$$

where ΔP is the pressure decrement, V_i is the specific volume on the isotherm T at pressure P_r ($=P_{mp}-\Delta P$), and we again take $\gamma/\gamma_o = (V/V_o)^n$. The energy change from (V_{mp},P_{mp}) to (V_i,P_r) along the adiabat is

$$\Delta E_a = \Delta P(V_r - V_{mp})/2 + C_p T\left(1-\exp[\gamma_o(V_{mp}^n - V_r^n)/n/V_o^n]\right) \quad (7)$$

where V_r is the specific volume on the adiabat at P_r. The second term in (7) is the energy change at constant pressure from the adiabat to the isotherm, $C_p(T-T_s)$, where T_s is the adiabat temperature (equation (5)) at P_r. C_p is related to C_v by

$$C_p = C_v(1+\alpha\gamma T) \quad (8)$$

where α is the volume thermal expansion coefficient, which we approximate as

$$\alpha = \gamma C_v \rho/K_T \approx C_v(\Delta\rho/\Delta P)_T \quad (9)$$

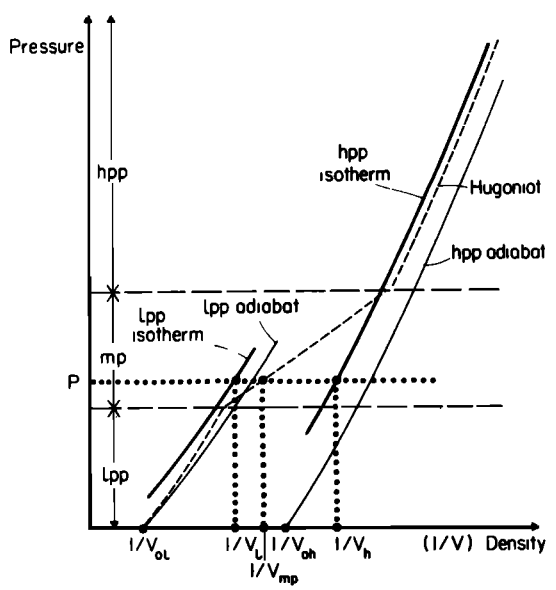

Fig. 2. Schematic diagram of the iterative calculation of release adiabats from mixed-phase Hugoniot pressure P_{mp} using energy balance conditions in equations (6) and (7). The figure illustrates the first iteration.

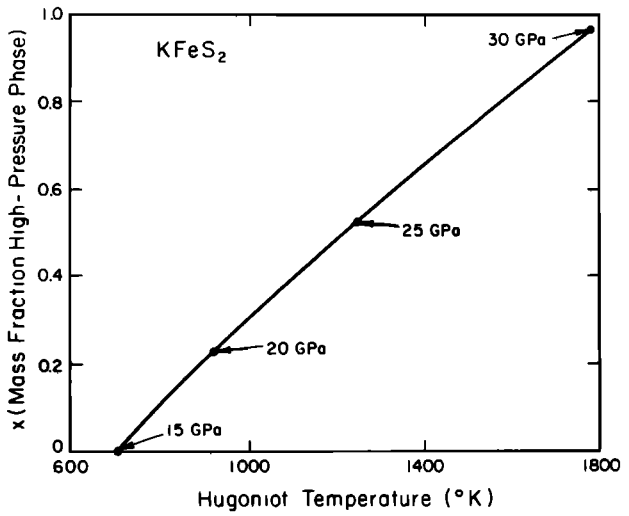

Fig. 3. Calculated mass fraction x of the high-pressure phase versus Hugoniot temperature T in the mixed-phase region of potassium thioferrite between 15 and 30 GPa.

Equating energy changes along the two paths (equations (6) and (7)) gives an implicit equation for the specific volume V_r at P_r on the release adiabat, which we solve numerically for the lpp and hpp separately. The V_r values for both phases are then combined using (1) to yield the density on the mp release adiabat at P_r. Because lpp and hpp release adiabats at P_r are at different temperatures (equation (5)), we take the temperature at P_r on the release adiabat as

$$T_r(P_r) = xT_{sh} + (1-x)T_{s\ell} \quad (10)$$

thus assuming that thermal equilibrium is maintained between the two phases with equal heat capacities along the release path. The release path point (V_r,P_r) is then taken as a new mp starting point, and the process is repeated (with $T=T_r$) until $P_r = 0$. We generally divide P_{mp} into 10 equal intervals for the release adiabat computation.

Results for $KFeS_2$ and $Fe_{0.9}S$

We illustrate the above method with potassium thioferrite, $KFeS_2$, and pyrrhotite, $Fe_{0.9}S$. These materials were chosen because shock wave data are available that include several mp Hugoniot states [Somerville and Ahrens, 1980; Ahrens, 1979]. For $Fe_{0.9}S$ [Ahrens, 1979], partial release states also were reported from buffer mirror measurements. Partial release states were not given for $KFeS_2$ [Somerville and Ahrens; 1980]; however, we have extracted release states from the original streak records, as described below.

We first consider $KFeS_2$. In Figure 3 we plot the mass fraction x of high-pressure phase versus Hugoniot temperature for the mp region, using the approach described above. The lpp and hpp EOS parameters are those in Table 3 of Somerville and Ahrens [1980] for third-order finite strain fits to the lpp and hpp data. There is a nearly linear variation of x with isotherm temperature. For mp Hugoniot pressures from 15 to 30 GPa, x increases from 0 to 0.97, i.e., from no hpp component to

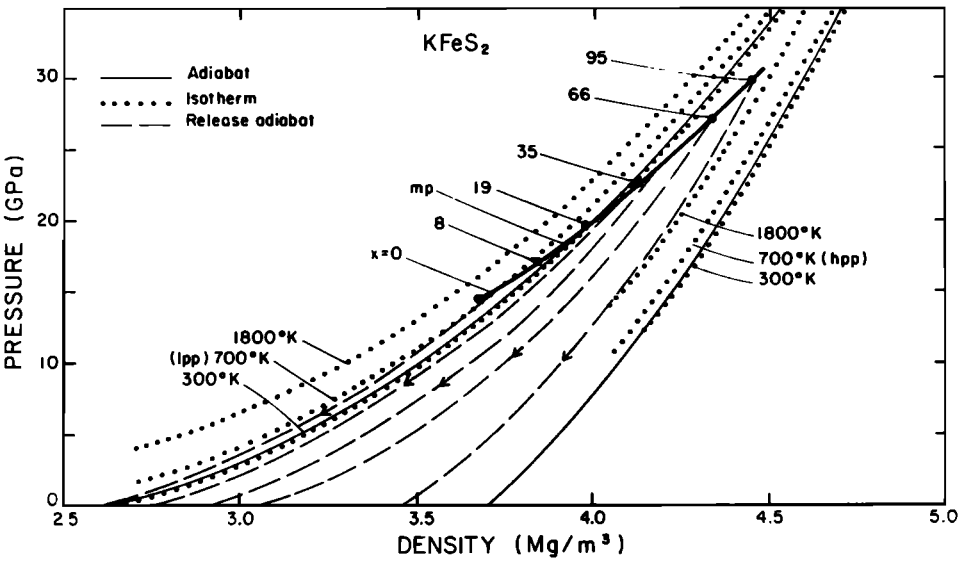

Fig. 4. Calculated frozen concentration release adiabats (dashed lines) for $KFeS_2$ in the mixed-phase regime for Hugoniot pressures of 15, 21, 24, 27, and 30 GPa. The heavy line is a quadratic P-ρ fit to the mixed-phase Hugoniot states. The mass fraction x of high-pressure phase is indicated for each mixed-phase Hugoniot point. Also shown are adiabats (thin lines) and 300, 700, and 1800°K isotherms (dotted lines) of the low- and high-pressure phases of $KFeS_2$ calculated using the equation of state parameters of Somerville and Ahrens [1980].

nearly complete conversion. Thus the mp region proposed by Somerville and Ahrens and the fitted EOS parameters are consistent with our calculated proportions of lpp and hpp, although we would begin the mp regime at 15 GPa rather than at 13 GPa as suggested by Somerville and Ahrens. For Hugoniot pressures below 15 GPa our calculations yield negative values for x.

Zou et al. [1982] carried out a static compression study of $KFeS_2$ to 34.5 GPa. The data are consistent with the shock wave results of Somerville and Ahrens [1980] except that three distinct phases were observed: a low-pressure phase stable to 15.8 GPa, a high-pressure phase stable from 15.8 to 27.4 GPa, and a second high-pressure phase stable above 27.4 GPa.

Figure 4 shows calculated release adiabats for the $KFeS_2$ mp region calculated by the iterative method described above. The heavy curve through the mp points is a quadratic least squares fit in density: $P(GPa)=36.22-26.99\rho+5.72\rho^2$ (ρ in Mg/m^3). The mp Hugoniot pressures have been corrected for porosity, ranging between 1.1 and 3.8%, as described by Jeanloz [1979]. This correction reduces Hugoniot pressures reported by Somerville and Ahrens [1980] by 0.2-0.5 GPa. Included in Figure 4 are adiabats and 300, 700, and 1800°K isotherms for both the lpp and hpp. All curves were calculated from the EOS data in Table 3 of Somerville and Ahrens [1980]. Also shown are our calculated release adiabats for mp Hugoniot pressures of 15, 21, 24, 27, and 30 GPa. The theoretical release paths become shallower as mp Hugoniot pressures decrease, in agreement with the results of Ahrens and Rosenberg [1968] and Grady et al. [1974] on quartz. This is a consequence of the steeper slope of the hpp adiabat.

In order to compare theoretical release adiabats and measured release paths we have reanalyzed the shock wave streak records for $KFeS_2$ and extracted partial release states, given in Table 1. Our values for initial densities, projectile velocities, and shock wave velocities agree with those in Table 2 of Somerville and Ahrens [1980] within one standard error, except for shots LGG54 and LGG56 (hpp region) where we agree within two standard errors. The partial release states are determined from shock wave velocities measured in buffer mirrors of fused quartz or lexan on the $KFeS_2$ samples and the impedance matching method [Walsh and Christian, 1955]. Buffer mirror equation of state data used were those of Wackerle [1962] and Jackson and Ahrens [1979] for fused quartz and Carter and Marsh [1977] for lexan. In Table 2 we list our measured buffer shock wave velocity u_B, the Hugoniot state (particle velocity u_p^H, pressure P^H, and density ρ^H) as given by Somerville and Ahrens, and our values for the partial release states (u_p^R, P^R, and ρ^R).

We plot Hugoniot and release states in Figure 5 for pressures up to 50 GPa, excluding the two highest pressure points at 100 and 111 GPa. On the basis of shock velocity/particle velocity plots and fitted lpp and hpp equations of state, Somerville and Ahrens concluded that the mp regime extends from about 13 to 30 GPa. In this region of Figure 5 the partial release states lie on the Hugoniot, within the experimental error. At the lowest Hugoniot pressures (1.6 and 4.3 GPa), the samples unload at almost constant density. In the high-pressure region the release path from 45 GPa is much shallower than the Hugoniot. Similar behavior occurs for the 100- and 111-GPa Hugoniot points. We emphasize that because of the method of calculating the Riemann integral the partial release paths yield maximum partial release densities (maximum release path slopes). Comparing Figures 4 and 5, we can conclude that since the measured partial release paths are much shallower than the theoretical re-

TABLE 1. Measured Buffer Shock Wave Velocities and Calculated Hugoniot and Partial Release States for $KFeS_2$

Shot	u_B, km/s	Hugoniot State u_p^H, km/s	p^H, GPa	ρ^H, Mg/m^3	Partial Release State u_p^R, km/s	p^R, GPa	ρ^R, Mg/m^3
451	2.647 (±0.022)	0.223 (±0.004)	1.56 (±0.04)	2.78 (±0.04)	0.20 (±0.01)	0.64 (±0.05)	2.78 (±0.01)
444	3.199 (±0.020)	0.515 (±0.005)	4.27 (±0.04)	3.06 (±0.04)	0.55 (±0.01)	2.12 (±0.06)	3.05 (±0.01)
450	3.626 (±0.024)	0.630 (±0.010)	5.55 (±0.11)	3.17 (±0.05)	0.83 (±0.01)	3.58 (±0.08)	2.98 (±0.02)
455	3.621 (±0.025)	0.635 (±0.002)	5.76 (±0.04)	3.18 (±0.03)	0.82 (±0.02)	3.56 (±0.09)	3.02 (±0.03)
440	4.097 (±0.029)	0.851 (±0.002)	8.29 (±0.06)	3.38 (±0.03)	1.13 (±0.02)	5.51 (±0.13)	3.10 (±0.05)
437	4.542 (±0.069)	1.06 (±0.02)	11.4 (±0.3)	3.50 (±0.07)	1.41 (±0.04)	7.65 (±0.36)	3.18 (±0.10)
458	4.892 (±0.040)	1.31 (±0.01)	14.6 (±0.1)	3.67 (±0.04)	1.63 (±0.03)	9.55 (±0.23)	3.39 (±0.05)
470	5.181 (±0.044)	1.45 (±0.01)	17.2 (±0.2)	3.83 (±0.05)	1.82 (±0.03)	11.2 (±0.3)	3.49 (±0.06)
467	5.480 (±0.047)	1.63 (±0.01)	19.7 (±0.2)	3.97 (±0.03)	2.01 (±0.03)	13.1 (±0.3)	3.64 (±0.06)
436	5.826 (±0.052)	1.79 (±0.04)	22.5 (±0.5)	4.13 (±0.08)	2.23 (±0.03)	15.5 (±0.4)	3.73 (±0.08)
435	6.289 (±0.059)	2.05 (±0.05)	27.4 (±0.7)	4.34 (±0.09)	2.52 (±0.04)	19.0 (±0.5)	3.88 (±0.09)
449	---	2.16 (±0.01)	30.0 (±0.3)	4.47 (±0.04)	---	---	---
LGG56	5.585 (±0.051)	2.79 (±0.02)	45.1 (±0.6)	4.68 (±0.06)	2.82 (±0.03)	34.7 (±0.7)	4.27 (±0.03)
LGG54	8.781 (±0.113)	4.45 (±0.02)	100.3 (±1.1)	5.30 (±0.07)	4.84 (±0.07)	93.6 (±2.6)	4.75 (±0.25)
LGG69	9.262 (±0.091)	4.72 (±0.02)	111.1 (±1.3)	5.40 (±0.08)	5.14 (±0.06)	104.9 (±2.2)	4.26 (±0.26)

Shot numbers refer to Table 2 of Somerville and Ahrens [1980], which gives initial densities and projectile and sample shock wave velocities.

lease adiabats, the $KFeS_2$ phase transformation must begin reversing as soon as the samples start to unload.

Complete release states were obtained for seven shots with Hugoniot pressures below 30 GPa using inclined mirrors on the $KFeS_2$ samples [Ahrens et al., 1968]. Zero-pressure release densities from pressures of 4.27, 5.55, 5.76, 8.29, 14.6, 17.2, and 19.7 GPa are 2.06, 2.59, 2.60, 2.65, 2.33, 2.37, and 2.59 Mg/m^3, respectively. The average, 2.46(±0.15) Mg/m^3, is close to the initial density of $KFeS_2$ (2.663 Mg/m^3).

TABLE 2. Equation of State Data for $Fe_{0.9}S$

	Low-Pressure Phase	High-Pressure Phase A	High-Pressure Phase B
ρ_o, Mg/m^3	4.6025	5.54	5.3
K_o, GPa	55.	150.	106.
K_o', dimensionless	4.0	4.2	4.9
E_{tr}, kJ/g	0.0	0.097	0.097
γ_o, dimensionless	1.13	1.3	1.3
n, dimensionless	1.0	1.0	1.0

Column B gives the hpp preferred values.

We note that in the iterative energy balance procedure for calculating the theoretical release paths (equations (6) and (7)) the differences between the isothermal and adiabatic release paths from a given pressure are negligible (0.001 Mg/m^3 or less). This would be expected from the essentially parallel nature of the adiabats and isotherms in Figure 4. The release path calculation (Figure 2) shifts the adiabat to lower densities to intersect the isotherm at the required pressure, and thus the isothermal and adiabatic paths in Figure 2 should be nearly coincident. Accordingly, one can conclude that addition of adiabats used by Grady et al. [1974] for frozen concentration release paths is an excellent approximation. We note, however, that using adiabats to compute the mass fraction of high-pressure phase at a given mp pressure underestimates the mass fraction. For example, at 20 GPa, use of lpp and hpp adiabats to determine x yields an hpp mass fraction of 0.08 compared to the correct value of 0.22 derived from isotherms.

We now consider a case in which the mp analysis can be combined with hpp Hugoniot data to

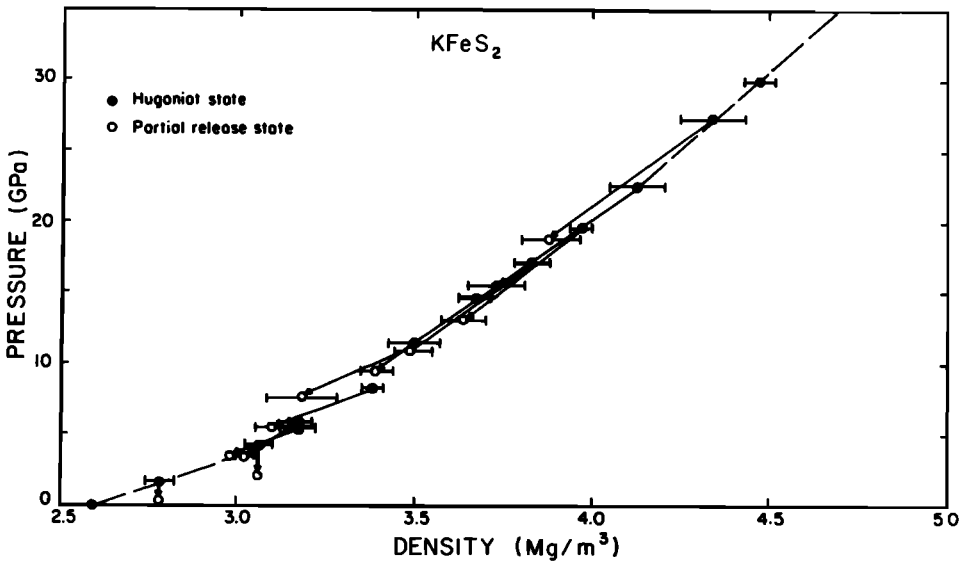

Fig. 5. Hugoniot (solid cicles) [Somerville and Ahrens, 1980] and partial release (open circles) states for $KFeS_2$. Partial release states are new data derived by rereading of the original streak records of Somerville and Ahrens.

constrain further hpp EOS parameters. We use as an illustration data of Ahrens [1979] for pyrrhotite, $Fe_{0.9}S$. We note at the outset that the hpp EOS parameters in Table 4 of Ahrens [1979] do not provide a good fit to the high-pressure data, as shown by the dashed curves in Figure 6.

We have done a third-order finite strain refit of the hpp data in Figure 6 and give the results in Table 2 (column A). The zero-pressure hpp density was taken as the maximum zero-pressure release density found from inclined mirrors on the samples using techniques described by Ahrens et al. [1969]. In shock wave reconnaissance experiments, where there exist no independent static compression determinations of the hpp zero-pressure density, one must make some such choice. In the discussion below we show how use of mp data confirms that this choice for zero-pressure hpp density is a poor one. The revised analysis for $Fe_{0.9}S$ yields a bulk modulus K_0 about 50 GPa higher than that previously reported, and a value of the first pressure derivative of K_0, K_0', about 0.6 lower.

In Table 2 we also include EOS parameters for the low-pressure phase of $Fe_{0.9}S$. The lpp values of K_0 and K_0' are based on measurements by N. I. Christensen (private communication, 1972). The only other measurements of pyrrhotite K_0 of which we are aware are those of Birch and Bancroft [1939] for a sample of unspecified composition with $\rho_0 = 4.587$ Mg/m^3 yielding K_0 values from 52 to 73 GPa.

In Figure 6 we also plot the measured partial release states from buffer mirror data and complete release states from inclined mirror observations. Again, we emphasize that these release paths yield maximum postshock densities. The release paths become shallower as Hugoniot pressure decreases, except for the release path from 29.1 GPa. It is evident in Figure 6 that the previous hpp results for $Fe_{0.9}$ are in error; however, one might wish a better fit between 30 and 50 GPa, even with the revised parameters. On the other hand, it would not be unreasonable to expect that the mp region might extend to these higher pressures. It is these possibilities that we use the mp region Hugoniot data to explore.

We calculate the fraction of hpp $Fe_{0.9}S$ in the mp regime using our revised hpp EOS parameters (Table 2, column A) and fitting the mixed-phase Hugoniot by a quadratic in density between 5 and 25 GPa, the mp region proposed by Ahrens [1979]. The results are plotted as the short-dashed line in Figure 7. Even at 25 GPa, only about 70% of

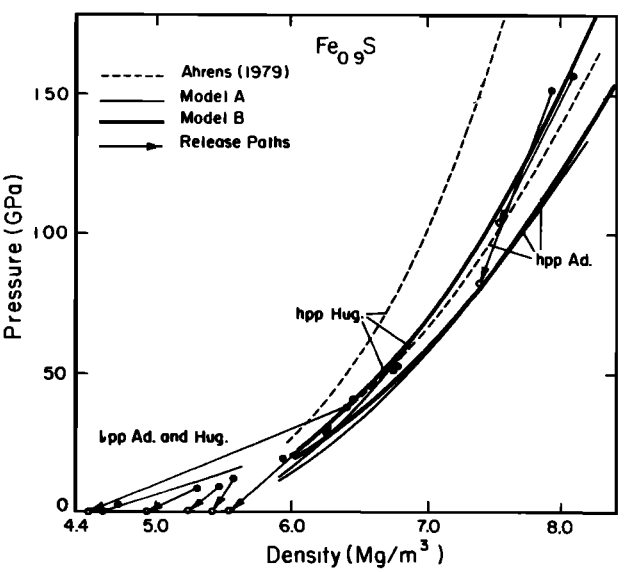

Fig. 6. Hugoniot (solid circles) and release (open circles) data for pyrrhotite, $Fe_{0.9}S$ [Ahrens, 1979]. Also shown are adiabats and Hugoniots calculated from the equation of state fit of Ahrens [1979] (dashed lines), our initial reanalysis of the high-pressure phase data (Table 2, column A), and our preferred analysis (Table 2, column B) including the mixed-phase region data (heavy curves).

the $Fe_{0.9}S$ appears to have transformed. Thus the hpp EOS parameters used in constructing the hpp Hugoniot in Figure 6 (model A) and the calculated proportion of hpp in the mixed-phase region are not consistent with each other. Either the hpp EOS parameters or the pressure limits of the mp regime are in error.

One obvious solution is to extend the mp region to higher pressures. Figure 6 suggests that using our revised hpp EOS parameters, the Hugoniot points at 29.1, 30.6, 38.7 and 40.7 GPa should perhaps belong in the mp region. Repeating the calculation of the proportion of the hpp in an mp regime from 5 to 40 GPa, with a new quadratic P-ρ fit, yields the long-dashed curve in Figure 7. This extended mp region requires that the amount of hpp in the mp region decreases once Hugoniot pressures exceed 30 GPa, an implausible result. Thus we can conclude that an extended mp regime is not acceptable, and we must attribute the difficulty to our model A EOS parameters and, specifically, to our choice of an hpp zero-pressure density. This conclusion would most likely not have been reached in the absence of both a static compression zero-pressure hpp density and our mixed-phase calculation.

We now must modify the hpp EOS parameters in light of the above results. If we lacked a static compression zero-pressure density for the hpp (as is the case in a reconnaissance experiment), we would most likely be inclined to lower the hpp density somewhat to yield a better fit to the Hugoniot data between 30 and 50 GPa, since we have shown that these points are not in the mp regime. In the present case, however, we note that independent static compression studies of troilite, FeS, have been done. Pichulo et al. [1976] observed a density increase of 16% in phase transitions in troilite from FeS(I) to FeS(III). The transition from FeS(I) to FeS(II) was a minor transformation with a density increase of about 1%, while the FeS(II)→FeS(III) transition had a density increase of about 15%. Recently, Mao et al. [1981] refined the structure of the highest FeS phase, FeS(IV), from diamond cell static compression data from 15 to 60 GPa and found disagreement with Pichulo et al.'s FeS(IV) orthorhombic lattice parameters. Mao et al. found the net density change from FeS(I) to FeS(IV) to be 15.7%. By analogy we take a zero-pressure hpp density of 5.3 Mg/m^3 for pyrrhotite, an increase of 15% relative to the lpp zero-pressure density.

The results of the new fit to the Hugoniot data above 30 GPa are given in column B of Table 2. Compared to model A, K_0 is reduced by 46 GPa, and K_0' is increased by 0.7. For comparison, Mao et al. [1981] determined K_0 for FeS(IV) as 137 GPa using a Murnaghan EOS with $K_0'=4$. Our hpp adiabat and Hugoniot curves from model B are plotted as the heavy lines in Figure 6 and are an improved fit to the Hugoniot data between 30 and 50 GPa. The proportion of high-pressure phase calculated using these new EOS parameters is plotted as the solid curve in Figure 7. The results show that at 27 GPa, nearly all the $Fe_{0.9}S$ has transformed to the hpp and that the mixed-phase region extends from just below 5 GPa to just above 27 GPa. Thus the revised hpp EOS values and the mixed-phase regime calculations are consistent, and the disagreements between the two regions found with the model A hpp parameters have been eliminated.

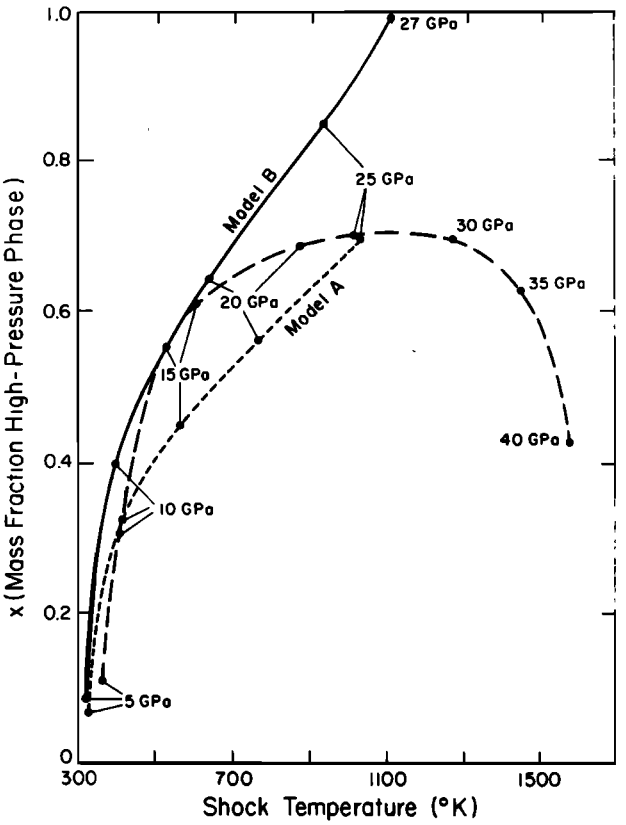

Fig. 7. Computed mass fraction of high-pressure phase for pyrrhotite in the mixed-phase regime. The long-dashed curve uses the same equation of state parameters as the short-dashed curve but extends the mixed-phase region to 40 GPa. Above Hugoniot pressures of about 30 GPa, the amount of high-pressure phase decreases, an inconsistent result. The solid, preferred curve is calculated using equation of state parameters of Table 2, column B, and indicates that complete transformation occurs at 27 GPa.

In Figure 8, we plot calculated release adiabats for mp Hugoniot pressures of 5, 9, 15, 23, and 27 GPa. We also include lpp and hpp adiabats and 300 and 1200°K isotherms. The heavy line is a quadratic P-ρ fit to the mp Hugoniot points: $P(GPa)=198.82-85.17\rho+9.28\rho^2$ (ρ in Mg/m^3). As was the case with $KFeS_2$, the calculated release adiabats become shallower at lower mp Hugoniot pressures. The measured release adiabats in the mp region are all much steeper than the theoretical release paths. Since, as we have noted, the measured release paths yield only maximum postshock densities, the results are not inconsistent with our calculated curves.

Summary

We have considered materials that show phase transformations upon shock compression and have formulated a method for calculating the amount of high-pressure phase in the mixed-phase regime as an additional test for equation of state parameters of the high-pressure phase derived from the Hugoniot states. Using EOS parameters for the individual low- and high-pressure phases, we com-

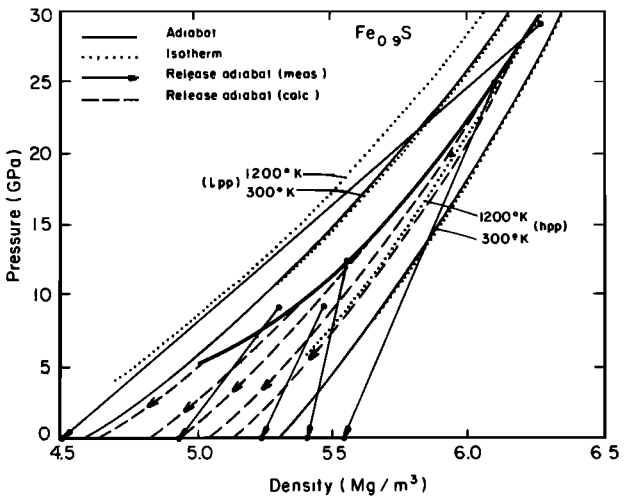

Fig. 8. Calculated frozen concentration release adiabats (dashed lines) for unloading from $Fe_{0.9}S$ mixed-phase Hugoniot pressures of 5, 9, 15, 23, and 27 GPa. The heavy line is a quadratic P-ρ fit to the mixed-phase Hugoniot data. Also plotted are adiabats (thin lines) and 300 and 1200°K isotherms (dotted lines) for the low- and high-pressure phases computed from our preferred parameters (Table 2, column B).

bine isotherms of the two phases and use mass and energy balance conditions to determine relative proportions of the two phases on the Hugoniot throughout the mixed-phase region. By so doing, we assume pressure, temperature, and particle velocity equilibrium between the two phases. We can then apply two simple requirements for the calculated proportion of high-pressure phase in the mp region: (1) it must increase monotonically with increasing Hugoniot pressure, and (2) it must approach one at the high-pressure end of the mixed-phase regime. Thus Hugoniot data from the mp region, which have usually been regarded as of no particular use other than to fix in a general way the pressure at which the transition to the high-pressure phase is completed, can be used quantitatively in conjunction with the high-pressure region Hugoniot data in constraining equation of state parameters.

Our calculations for the potassium thioferrite mixed-phase region show that the hpp EOS parameters of Somerville and Ahrens [1980] are consistent with a mixed-phase region extending from 15 to 30 GPa. The release paths determined from the original $KFeS_2$ shock records show that as unloading begins from Hugoniot states in the mp region, the transformation reverses. Our computed release paths for frozen concentration (fixed concentration of low- and high-pressure phases coexisting at a given Hugoniot pressure) are considerably steeper than the measured release paths.

We have used our analysis of the mixed-phase regime to refine the high-pressure EOS parameters of pyrrhotite reported by Ahrens [1979]. Fitting the high-pressure Hugoniot data without using data from the mixed-phase region leads to an inconsistent result that either only about 70% of the material has transformed at the upper end of the presumed mp region or, if the mixed-phase regime is extended to higher pressures, the proportion of high-pressure phase begins decreasing once Hugoniot pressures exceed about 30 GPa. This illustrates the difficulties one can encounter in shock wave reconnaissance experiments, where no independent measurement of the zero-pressure density of the high-pressure phase exists and where only high-pressure region Hugoniot data, and not the mixed-phase region states, are used to fit equations of state.

By adjusting the high-pressure EOS parameters we can simultaneously fit the high-pressure region Hugoniot data and achieve monotonically increasing proportions of the high-pressure phase in a mixed-phase region extending from just below 5 GPa to just above 27 GPa, with the proportion of hpp approaching unity at the high-pressure end of the mp regime. Revised values for the zero-pressure density, bulk modulus and first pressure derivative of the the bulk modulus of the high-pressure phase of $Fe_{0.9}S$ are 5.3 Mg/m^3, 106 GPa, and 4.9, respectively.

This technique should be especially useful in shock reconnaissance work, where data for the zero-pressure density of high-pressure phases are not available from other methods, and should provide motivation for acquiring additional, useful Hugoniot data in the mixed-phase regime.

Acknowledgments. We appreciate discussions with M. B. Boslough and J. M. Vizgirda as well as a helpful review from J. M. Brown. Computing support was provided by the Office of Computer Services and the Department of Geology, Rensselaer Polytechnic Institute. Supported by NSF grant EAR 79-26384. Contribution 3733, Division of Geological and Planetary Sciences, California Institute of Technology.

References

Ahrens, T. J., Equations of state of iron sulfide and constraints on the sulfur content of the Earth, J. Geophys. Res., 84, 985-998, 1979.

Ahrens, T. J., and J. T. Rosenberg, Shock metamorphism: Experiments on quartz and plagioclase, in Shock Metamorphism of Natural Materials, edited by B. M. French and N. M. Short, pp. 59-81, Mono Book Corp., Baltimore, Md., 1968.

Ahrens, T. J., W. H. Gust, and E. B. Royce, Material strength effect in the shock compression of alumina, J. Appl. Phys., 39, 4610-4616, 1968.

Ahrens, T. J., C. F. Petersen, and J. T. Rosenberg, Shock compression of feldspars, J. Geophys. Res., 74, 2727-2746, 1969.

Ahrens, T. J., F.-D. Tsay, and D. H. Live, Shock-induced fine-grained crystallization of olivine: Evidence against subsolidus reduction of Fe^{2+}, Proc. Lunar Sci. Conf., 7th, 1143-1156, 1976.

Birch, F., and D. Bancroft, The elasticity of certain rocks and massive minerals, Am. J. Sci., 237, 2-6, 1939.

Carter, W. J., and S. P. Marsh, Hugoniot equations of state of polymers, Rep LA-UR-77-2062, Los Alamos Natl. Lab., Los Alamos, N. M., 1977.

Grady, D. E., Processes occurring in shock wave compression of rocks and minerals, in High-Pressure Research: Applications in Geophysics,

edited by M. H. Manghnani and S. Akimoto, pp. 389-438, Academic, New York, 1977.

Grady, D. E., Shock deformation of brittle solids, J. Geophys. Res., 85, 913-924, 1980.

Grady, D. E., W. J. Murri, and G. R. Fowles, Quartz to stishovite: Wave propagation in the mixed phase region, J. Geophys. Res., 79, 332-338, 1974.

Jackson, I., and T. J. Ahrens, Shock wave compression of single-crystal forsterite, J. Geophys. Res., 84, 3039-3048, 1979.

Jeanloz, R., Properties of iron at high pressures and the state of the core, J. Geophys. Res., 84, 6059-6069, 1979.

Jeanloz, R., and T. J. Ahrens, Pyroxenes and olivines: Structural implications of shock-wave data for high-pressure phases, in High-Pressure Research: Applications in Geophysics, edited by M. H. Manghnani and S. Akimoto, pp. 439-461, Academic, New York, 1977.

Jeanloz, R., and T. J. Ahrens, Release adiabat measurements on minerals: The effect of viscosity, J. Geophys. Res., 84, 7545-7548, 1979.

Jeanloz, R., and T. J. Ahrens, Anorthite: Thermal equation of state to high pressures, Geophys. J. R. Astron. Soc., 62, 529-549, 1980.

Kieffer, S. W., and J. M. Delaney, Isentropic decompression of fluids from crustal and mantle pressures, J. Geophys. Res., 84, 1611-1620, 1979.

Lyzenga, G. A., and T. J. Ahrens, The relation between the shock-induced free-surface velocity and the postshock specific volume of solids, J. Appl. Phys., 49, 201-204, 1978.

Mao, H. K., G. Zou, and P. M. Bell, High-pressure experiments on FeS with bearing on the composition of the earth's core, Year Book Carnegie Inst. Washington, 1980, 267-272, 1981.

McQueen, R. G., S. P. Marsh, and J. N. Fritz, Hugoniot equation of state of twelve rocks, J. Geophys. Res., 72, 4999-5036, 1967.

Pichulo, R. O., T. Takahashi, and J. S. Weaver, High pressure polymorphism of FeS (abstract), Eos Trans. AGU, 57, 340, 1976.

Rice, M. H., R. G. McQueen, and J. M. Walsh, Compression of solids by strong shock waves, Solid State Phys., 6, 1-63, 1958.

Somerville, M., and T. J. Ahrens, Shock compression of $KFeS_2$ and the question of potassium in the core, J. Geophys. Res., 85, 7016-7024, 1980.

Wackerle, J., Shock-wave compression of quartz, J. Appl. Phys., 33, 922-937, 1962.

Walsh, J. M., and R. H. Christian, Equation of state of metals from shock wave measurements, Phys. Rev., 97, 1544-1556, 1955.

Watt, J. P., and T. J. Ahrens, Shock compression of single-crystal forsterite, J. Geophys. Res., 88, 9500-9512, 1983.

Zou, G., H. K. Mao, and P. M. Bell, High-pressure study of $KFeS_2$, Year Book Carnegie Inst. Washington, 1981, 277-279, 1982.

T. J. Ahrens, Seismological Laboratory, California Institute of Technology, Pasadena, CA 91125.

J. P. Watt, Department of Geology, Rensselaer Polytechnic Institute, Troy, NY 12181.

(Received September 13, 1982;
revised May 2, 1984;
accepted May 15, 1984.)